

Hydrothermal generation of hydrocarbons in basement rocks, Southern Tuscany



Andrea Schito¹, David Muirhead¹, Stephen Bowden¹ & John Parnell¹

¹ Department of Geology and Geophysics, School of Geosciences, University of Aberdeen, Aberdeen AB24 3UE, UK.

AS, [0000-0003-0760-9321](https://orcid.org/0000-0003-0760-9321); DM, [0000-0003-2065-6042](https://orcid.org/0000-0003-2065-6042); SB, [0000-0002-6370-8175](https://orcid.org/0000-0002-6370-8175).

Ital. J. Geosci., Vol. 141, No. 2 (2022), pp. 231-244, 7 figs., 3 tabs., <https://doi.org/10.3301/IJG.2022.10>.

Research article

Corresponding author e-mail: andrea.schito@abdn.ac.uk

Citation: Schito A., Muirhead D., Bowden S. & Parnell J. (2022) - Hydrothermal generation of hydrocarbons in basement rocks, Southern Tuscany. Ital. J. Geosci., 141(2), 231-244, <https://doi.org/10.3301/IJG.2022.10>.

Associate Editor: Orlando Vaselli

Submitted: 23 July 2021

Accepted: 19 January 2022

Published online: 26 April 2022

ABSTRACT

Carbonaceous material in the form of graphitic carbon, amorphous carbon and liquid hydrocarbons occurs in the metamorphic rocks of Monti Romani in Southern Tuscany. Raman spectroscopic analyses show a contrast in structural ordering between carbon in the host rocks and carbon films and nodules at the contact with high temperature mineralized veins. Microscopy and gas chromatography additionally indicate liquid hydrocarbons, with a thermal maturity at the peak of the oil window. The association of hydrocarbons with high temperature fluids together with gas chromatographic and spectroscopic data indicate a probable hydrothermal origin of the oils, from the late Miocene sediments that fill the Tafone Graben. A model is proposed in which hydrocarbons were generated along the fault that borders the Tafone Graben and then migrated toward the basement rocks at the footwall. The presence of 25-norhopane indicates biodegradation in the depth interval between about 100 and 1500 m. The hydrothermal generation of hydrocarbons could occur in other geothermal areas in Southern Tuscany where the presence of hydrocarbons has been reported but never fully explained.

KEY-WORDS: hydrothermal hydrocarbons, basement rocks, Raman spectroscopy, fluid inclusions, biomarkers.

INTRODUCTION

The occurrence of hydrocarbons in igneous and metamorphic rocks is widely recognized and reported in more than 100 countries around the world (Schutter, 2003). Such occurrences have commonly been regarded as evidence of abiogenic generation even if, in recent years it was demonstrated that, abiogenic hydrocarbons formed via Fischer-Tropsch reactions (Anderson et al., 1984) represent only a small proportion of the global budget in known reservoirs (Lollar et al., 2002). In basement reservoirs the source rocks do not necessarily lie beneath (Landes et al., 1960) and hydrocarbons often migrated downwards due to compactional squeezing of source rocks or laterally toward basement fault-bordered highs (Parnell 1988; Muirhead et al., 2017; Holdsworth et al., 2020).

Reservoirs hosted by volcanic rocks are also widespread in geothermal settings where hydrocarbons migrated from nearby source rocks that generated as a consequence of elevated temperature (Peabody, 1993; Schutter, 2003) or by the interaction of organic-rich rocks with hydrothermal fluids (Clifton et al., 1990; Schoell et al., 1990; Simoneit, 1990; Yamanaka et al., 2000; Venkatesan et al., 2003; Zárate-Del Valle & Simoneit, 2005; Zárate-Del Valle et al., 2006; Gurgey et al., 2007; Simoneit et al., 2009; Kontorovich et al., 2011). This phenomenon is often overlooked or underestimated in the geological record due to HC dispersion and/or migration (Parnell, 1988) or because of limited generation. In these cases it can be recognized by the occurrence of oil or degraded oil (i.e. bitumen) in fractures and/or mineralized veins. In veins, non-degraded oil can be generally recognized as UV-fluorescing inclusions in quartz



SOCIETÀ GEOLOGICA ITALIANA
Fondata nel 1881 - Ente morale R. D. 17 ottobre 1885



and calcite, while common modes of occurrence of bitumen are as nodules, as thin films along vein margins or around crystals, within vugs in breccia veins and fine disseminations within siliceous sinters (Peabody, 1993; Lindgren & Parnell, 2006). The importance of recognizing the generation and migration of petroleum residues and/or bitumen in hydrothermal areas is mainly because of their role in the uptake or reduction of metals during interaction with hydrothermal fluids to form ore deposits (Parnell, 1993).

Some of the most important ore mineralization in Italy is hosted in Southern Tuscany (Dessau et al., 1972), in particular in the Monte Amiata region (Brogi et al., 2011; Morteani et al., 2011; 2017; Rimondi et al., 2015), in the area of Boccheggiano (Liotta et al., 2010; Rossetti et al., 2011), in Gavorrano (Brogi et al., 2021) and in the Tafone Basin (Armiento et al., 2017). Mineralization is linked to the intense hydrothermal activity associated with Plio-Quaternary volcanism at the Tyrrhenian margin. Monte Amiata has been a major mercury producer until about thirty years ago (Brogi et al., 2011), being cited among the six most productive mines in the world (Brobst, 1973). The Boccheggiano area has also a long history of exploitation for pyrite, base metals and silver production, and important sulphide mineralization is recognized along the Pliocene Boccheggiano Fault (Liotta et al., 2010), while the Tafone Basin has been known as a mining district for sulphide epithermal minerals (stibnite and pyrite) since Etruscan times (VII-III centuries BC, Cipriani & Tanelli, 1983).

Throughout the area, the presence of hydrocarbons associated with mineralization has been noted by many authors (Arisi Rota & Vighi, 1971; Klemm & Neumann, 1984; Peabody, 1993; Rimondi et al., 2015; Biagioni et al., 2017; Morteani et al., 2017). These authors focus in particular on the presence of methane from gas emissions in the Mt. Amiata, Larderello, Manzianna and Latera geothermal systems (Peabody, 1993; Morteani et al., 2011; Tassi et al., 2012) and with heavy hydrocarbon occurrences in the deposits of Bagnore (SW of Mt. Amiata, Arisi Rota & Vighi, 1971; Klemm & Neumann, 1984; Rimondi et al., 2015; Biagioni et al., 2017). Even if most of the methane in the geothermal systems is thought to be abiogenic (Tassi et al., 2012), the origin of the heavy hydrocarbon is still unknown and has not yet been investigated in detail (Rimondi et al., 2015).

In this work we report for the first time evidence of hydrocarbons in the metamorphic rocks of Monti Romani at the footwall of the Tafone Basin, in Southern Tuscany, and attempt an understanding of the possible genesis, migration and degradation and the implications for ore deposits in similar areas.

GEOLOGICAL SETTING

The exhumed metamorphic units of the inner Northern Apennines cropping out in the area of Monti Romani is the focus of this study (Fig. 1a). The Northern Apennine fold and thrust belt formed as a consequence of the convergence between the Corsica-Sardinia block (European plate) and the Adria promontory (Adriatic plate) during the Late Miocene (Jolivet et al., 1998; Molli, 2008; Barchi, 2010). This process led to the stacking of units from different paleogeographic domains (i.e. Ligurian oceanic domain,

Tuscan epicontinental domain). In the Tuscan sector of the Northern Apennine the Paleozoic metamorphosed units are overthrust by the non-metamorphosed carbonate succession of the Tuscan Domain, which is in turn overthrust by the allochthonous Ligurian Units that represent the uppermost tectonostratigraphic unit of the northern Apennines (Brogi & Giorgetti, 2012). All of these units are unconformably covered by post-orogenic lower Miocene lacustrine and delta deposits (Cornamusini et al., 2011) and by Plio-Pleistocene marine and alluvial deposits. The exhumation of the metamorphic units is associated with a strong lithospheric thinning during Late Oligocene-Miocene extensional tectonics (Jolivet et al., 1998; Barchi, 2010). Since the Plio-Quaternary they were subjected to back-arc extension, with limited magmatism (Fig. 1a), there and along the whole Tyrrhenian margin (Accella & Funicello, 2006).

The studied area is located at the south-western border between Tuscany and Latium (Fig. 1a and b). In this locality, Roccaccia di Monteauto Fillades recently dated as Guadalupian by Molli et al., (2020), are mainly composed of dark metapelites and metarenites, which crop out on both flanks of the Tafone Graben and are overlain in tectonic contact (Brogi, 2008) by the dolomitic limestones of the Calcare Cavernoso Formation. The Tafone Graben infill is made up, from younger to older, by Plio-Pleistocene lacustrine sediments that lie unconformably on lower Miocene sandstones, conglomerates and shales that in turn unconformably cover the Ligurian and Tuscan Units (Fig. 1c, Moretti et al., 1990; Cornamusini et al., 2011). The thickness of the sediments above the Ligurian units never exceeds 200 m in the graben (Cornamusini et al., 2011).

Since the Miocene, the area experienced brittle tectonic deformation linked to extension and associated volcanism of the Tyrrhenian margin that led to the formation of the NW-SE faults that border the Tafone Graben and associated fractures and veins. Moreover, geothermal activity due to underlying magmatic bodies led to geothermal fluid circulation along the faults that border the graben. This activity is manifested as springs depositing travertine and epithermal stibnite and cinnabar mineralization (Morteani et al., 2011) in two abandoned mines in the area (Tafone and Monteauto mines, Fig. 1b).

MATERIALS AND METHODS

Materials

Six samples for organic geochemical and spectroscopic analyses on organic matter and four samples for fluid inclusions and petrographic observation on quartz were collected from an outcrop in Roccaccia di Monteauto locality (N 42°39'46,2" - E 11°35'56,5"; Figs. 1 and 2). Samples collected for geochemical analyses are composed of dark metapelites intensely deformed with a schistosity defined by the axial plane of isoclinal folds and a crenulation cleavage with a roughly NNW-SSE direction (black dotted lines in Fig. 2a). Brittle deformation is characterized by NW-SE faults (red dotted lines in Fig. 2a) and fractures.

The sampling strategy was to analyze organic-rich metapelites and quartz mineralization on a transect across the outcrop (Fig. 2a).

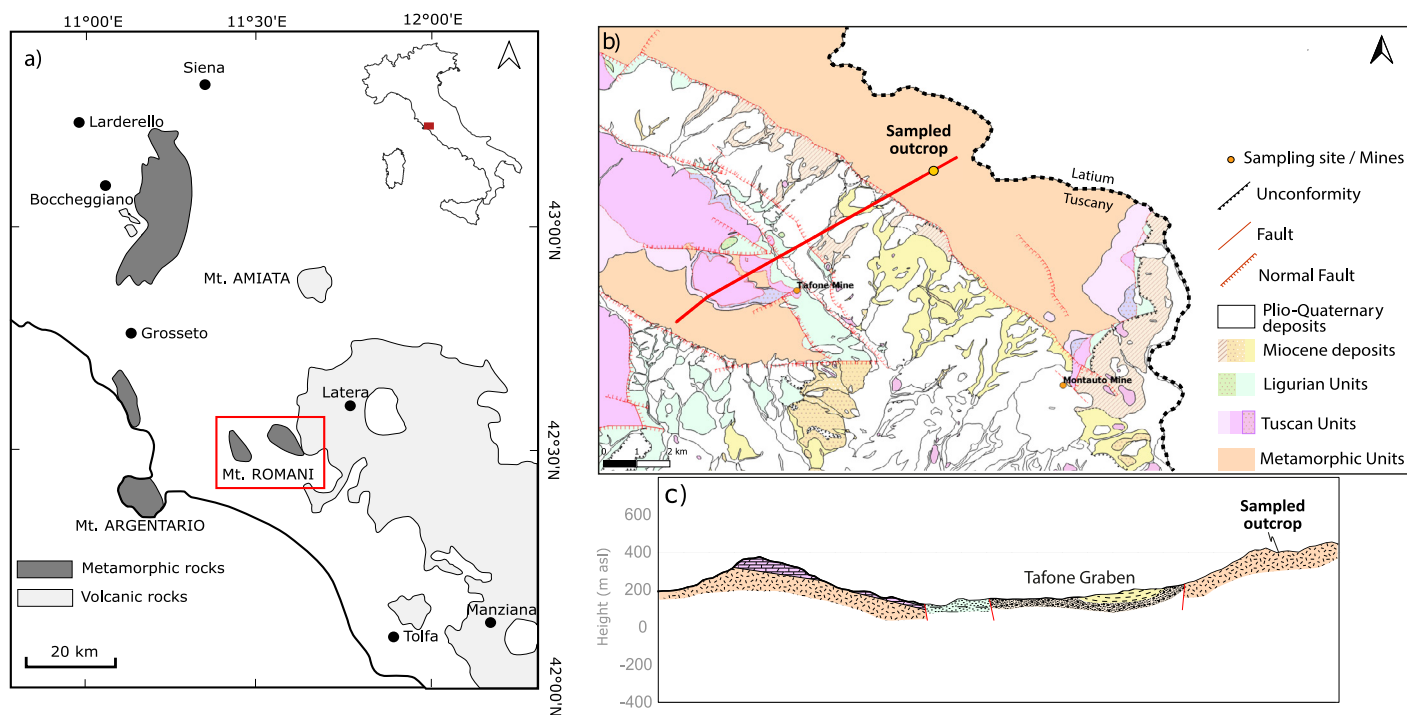


Fig. 1 - a) Metamorphic and volcanic outcrops in the Tuscan Tyrrenian margin; b) Geological map of the studied area showing sample location, mines location and section of geological profile; c) geological profile across the Tafone Graben. Geological map derived from Cornamusini et al. (2011) redrawn using the online database of Regione Toscana: <http://www502.regione.toscana.it/geoscopio/geologia.html>.

Figure 2b show an example of a vein samples for fluid inclusions analyses where the contact between quartz and pelites at the hinge of the fold is characterized by a dark film composed by carbonaceous material (Sample S15F).

Methods

Raman spectroscopy

Micro-Raman spectroscopy was carried out on metapelites cut perpendicular to the main foliation or perpendicular to the contact between the vein and the rock in sample S15F (see Fig. 2).

A Neodimium-Yag laser at 532 nm (green laser) in a backscattering geometry using a 600 grooves/mm spectrometer gratings and CCD detector was used. The instrument is equipped with 50× and 100× objective lens with a laser spot of about 2 μm diameter. An excitation wavelength of 532 nm with a power of 40 mW from an Ar⁺ laser was reduced up to 0.4 mW by using optical filters to avoid carbon overheating. Raman backscattered radiation was recorded for an integration time of 20s for 6 repetitions in a range between 700 and 2300 cm⁻¹. Depending on the spectra, Raman parameters were calculated by means of a four bands deconvolution suggested by Beyssac et al. (2002) for graphitic carbon or by the six bands deconvolution proposed by Schito et al. (2017) for diagenetic organic matter (Figs. 2d and e). Bands deconvolution was performed using LabSpec software by Horiba (Schito et al., 2017).

Fluid inclusion homogenization temperatures

Fluid inclusion analyses were performed on quartz veins as shown in Fig. 2a and c (samples SF1, SF2, SF3 and SF4). Samples

were prepared as 200 μm thick, doubly polished sections, then observed with a polarized microscope to define types of fluid inclusions and their genetic relationships. The homogenization temperatures of fluid inclusions were measured using a THMS-600 heating–freezing stage mounted on a Nikon Labophot transmission light microscope at the University of Aberdeen. The instrument is equipped with a range of objective lenses ranging from 20× to a 100× lens and was calibrated against synthetic H₂O (374.1 and 0.0 °C) and CO₂ (–56.6 °C) standards (Synthetic Fluid Inclusion Reference Set, Bubbles Inc., USA). The homogenization of aqueous two-phase inclusions was taken to indicate the temperatures at which the host mineral phase precipitated.

Gas Chromatography Mass Spectroscopy (GC-MS) analysis of biomarkers

Samples were solvent extracted using Soxhlet apparatus (about 10 g of rock was extracted in dichloromethane/methanol 93:7 v/v for 48 h). The extract was fractionated using flash mini-column chromatography (silica column; hexane for saturated fraction; 3:1 v/v hexane/dichloromethane for aromatics fraction; 2:1 v/v dichloromethane/methane for polar fraction). The resulting saturate fraction was analyzed by gas chromatography-mass spectrometry (GC-MS). GC-MS was performed using a 6890N Network GC system interfaced to a 5975 inert mass selective detector. A splitless injector (300°C) mode was used, and the GC temperature program was as follows; 60°C to 120°C at 20°Cmin⁻¹ then from 120°C to 290°C at 4°Cmin⁻¹. The column was Greyhound GC-5 (an HP-5 equivalent phase; 30 m length, 250 μm ID and 0.25

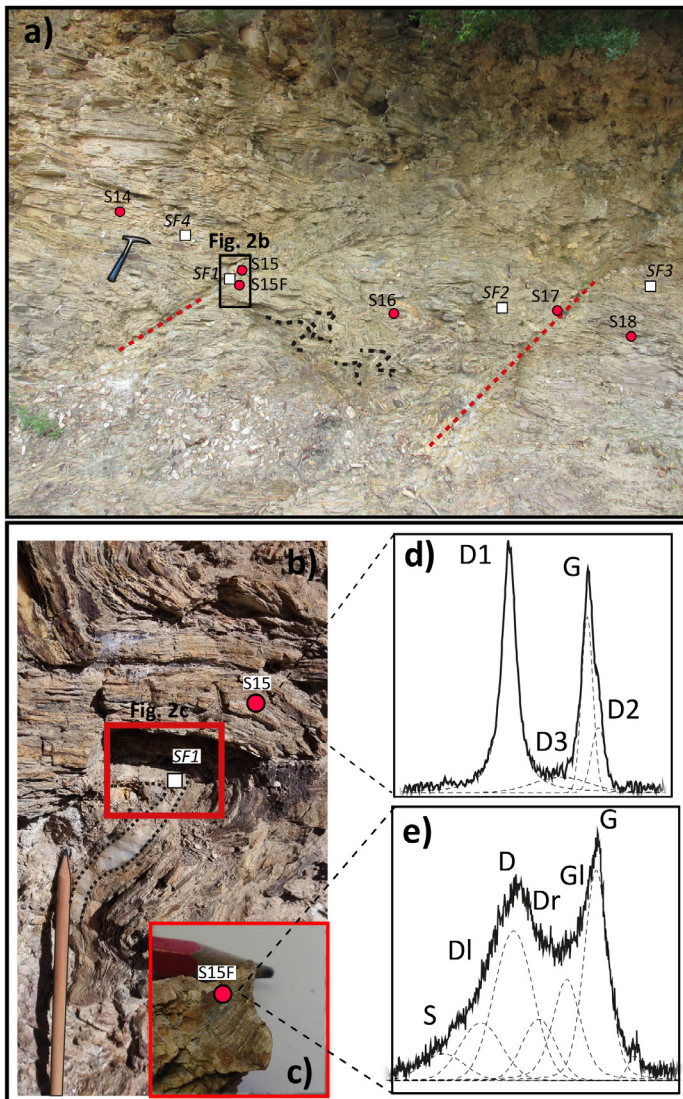


Fig. 2 - a) Photo of the sampled outcrop with normal faults highlighted with red-dotted lines and schistosity with black-dotted lines. Hammer length is 33 cm. Red dots indicates samples used for the analyses of the organic fraction (Raman and GC-MS) while white squares the location of veins for fluid inclusions analyses. b) Enlarged view of the black rectangle in Fig. a showing the quartz vein (black-dotted line) at the core of the fold. Pencil length is about 18 cm. c) The hinge of the fold in Fig. 2b is characterized by a dark film composed of carbonaceous material; d) Raman spectrum of graphitic carbon in the rocks (sample S15); e) Raman spectrum of disordered carbonaceous material that composed the dark film in Fig. 2c (Samples S15F). Raman bands in Fig. d are named after [Beysac et al. \(2002\)](#), while in Fig. e after [Schito et al. \(2017\)](#).

μm film thickness). The MS was operated in sim mode (less than 20 ions with a dwell time less than 40 ms).

RESULTS

Organic matter petrography and Raman Spectroscopy

Metapelites in southern Tuscany are characterized by a relatively high content in carbonaceous material that, in the area of Mte. Amiata, has been estimated to be 0.7% ([Elter & Pandeli, 1991](#); [Orlando et al., 2010](#)). At the macroscale, graphitic carbon grows parallel to schistosity (Fig. 2b and d) while amorphous

carbon occurs as dark films (Fig. 2c and e). At the microscale, thin sections show amorphous carbon generally occurs as nodules. Detailed SEM observations at the margin of quartz veins reveal that carbonaceous material occurs as: i) elongated fragments growing in clay-rich layers parallel to the foliation (Fig. 3a); ii) fractures or void-filling solid material (Fig. 3b and c) and iii) liquid hydrocarbons around quartz grains (Fig. 3d). Interestingly type ii and iii CM occur only just at the contact or inside the quartz veins.

Raman spectra of graphitic carbon are characterized by broad D and G bands, respectively at 1350 and 1600 cm^{-1} (Fig. 2d). The G band peak has an asymmetric shape due to the presence of the D2 band at about 1620 cm^{-1} and has similar intensities to the D band (Fig. 3b). A fourth broad band (D3 according to [Beysac et al., 2002](#)) lies in between the D and the G bands. In order to calculate maximum temperatures from Raman spectra, R2 parameter and paleotemperatures were calculated for each sample, according to [Beysac et al. \(2002\)](#), showing values between about 370 and $405\text{ }^{\circ}\text{C}$ (Table 1).

Amorphous carbon was found only in samples S15F and S17 with a spectrum composed by six first order bands between 1100 and 1700 cm^{-1} (Fig. 2e) and a broad signal in the second order Raman spectrum between 2650 and 2950 cm^{-1} . The first order spectrum is the result of the overlapping of several bands. The main bands are the D and G peaks, respectively at 1350 and 1600 cm^{-1} . The $\sim 1600\text{ cm}^{-1}$ graphite peak is a composite of several Raman bands at $\sim 1615\text{ cm}^{-1}$ and $\sim 1598\text{ cm}^{-1}$ that cannot be separated in poorly organised carbon or low-grade rocks ([Beysac et al., 2002](#)), such as those in this study. A further band at 1540 cm^{-1} (GI) contributes a left shoulder to the G band while a very small band occurs at 1700 cm^{-1} (Fig. 3d). The D band is bordered by two bands at around 1250 and 1500 cm^{-1} (Dr and DI according to [Li, 2007](#)) while a further band is found at a lower wavelength (S band at 1150 cm^{-1} ; [Li, 2007](#); [Deldicque et al., 2016](#); [Ferralis et al., 2016](#); [Schito et al., 2017](#); [Nirrengarten et al., 2020](#)). The main differences with graphitic carbon are evident by comparing the position and full width at maximum height (FWMH) of the G band (Tab. 1). In amorphous carbon the G band lies between 1606 and 1609 cm^{-1} with a FWHM of more than 80 cm^{-1} while it is closer to the graphite position at 1580 cm^{-1} and has a narrower FWHM in metamorphic organic matter (Tab. 1).

Moreover, Raman spectroscopy outline that, in all samples some black material (probably carbonaceous material) was recognized, but with a Raman spectrum totally overwhelmed by fluorescence (i.e., high hydrogen).

Gas-Chromatography Mass Spectrometry (GC-MS)

All samples and extracts contain a mixtures of recent and fossil (petroleum-like) organic matter (e.g. hydrocarbons from living organic matter as well as hydrocarbons found in petroleum). Both isoprenoid as well as lower carbon number n-alkanes (i.e. C_{16} to C_{22}) are the main constituents resolvable on the m/z 85 ion chromatograms of the hydrocarbon fractions. Where they are evident on chromatograms, high carbon n-alkanes have a strong odd over even preference indicating a mixture of surface biology (likely mosses or other endoliths – [Pancost et al., 2002](#))

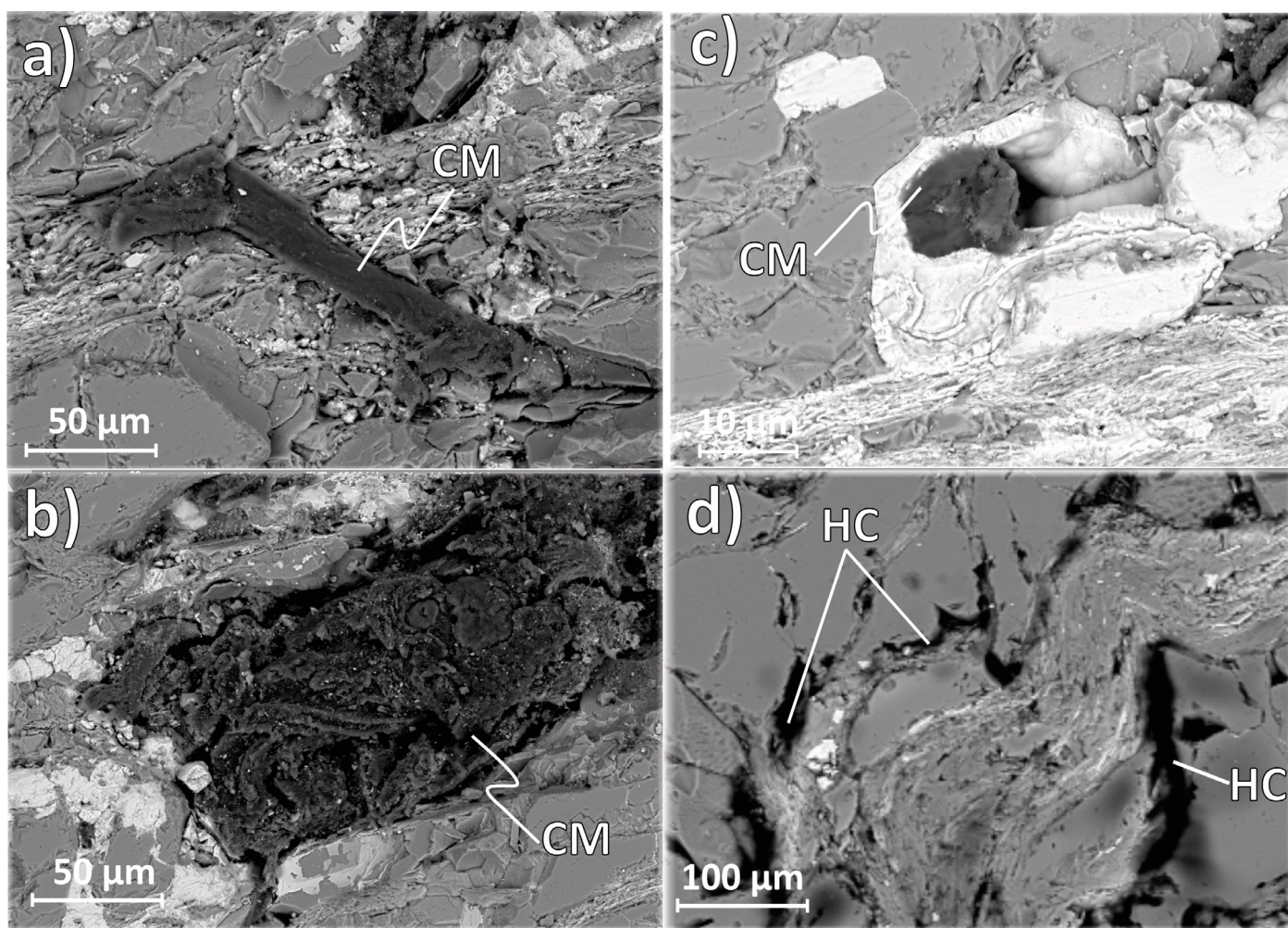


Fig. 3 - Back-scattered SEM images of carbonaceous material in the form of elongated fragments with smoothed surfaces (a); fracture filling solid material with some probable biological structures (b); hematite void filled by organic matter (c); liquid hydrocarbons around quartz grains (d). See materials section for more informations. CM – carbonaceous material; HC – hydrocarbons.

and petroleum n-alkanes. There are sufficient odd n-alkanes that they are unlikely to be attributable to biological sources alone (see [Parnell et al., 2008](#) for an example of naturally mixed petroleum and biological organic matter).

Similarly, triterpenoid and pentacyclic-terpenoid biomarkers also evidence inputs of both recent and fossil hopanoids, with many samples having diploptene as the main terpenoid (diploptene is a biomolecule not stable in the geological record, but biosynthesised by both mosses and prokaryotes, [Prahl et al., 1992](#)). However, some samples have a m/z 191 chromatogram far more typical of petroleum, in which diploptene is present in only very small amounts, with sample S15 exhibiting the distribution of hopanes most typical of geological samples. No samples contain high abundances of pre-oil window hopanoids, e.g. 17,21 β,β hopanes and neohop-17(21)-enes are not present; they evidence only directly biosynthesised hopanoids, or hopanoids found in oil produced during catagenesis. 25-Norhopanes are present in all samples, but are most clearly developed in sample S15, in terms of the presence of a range of carbon number homologues (up to 30) found in the regular hopanes (177 m/z ion chromatograms for hopanes and mass spectra for C_{29} 17 α 25-norhopane shown in Fig. 4).

The 25-norhopanes derive from the demethylation of regular hopanoids during biodegradation under subsurface conditions ([Bennett et al., 2006](#)). Although biodegradation does make petroleum viscous by removing lighter hydrocarbons ([Connan, 1984](#)), the mixing of light and heavier charges of oil means that oil containing biodegradation products can still be mobilised in the subsurface ([Parnell et al., 2017](#); [Al-Hajeri & Bowden, 2018](#)).

Steranes could also be detected in all samples but, relative to the hopanoids, characteristics indicative of biodegradation are not as clear; for example diasteranes and C_{29} regular steranes are not selectively enriched to a significant extent, which has been shown to happen during biodegradation at surface and near conditions (see [Parnell et al., 2017](#), for a case of biodegraded oil within basement rocks). Nevertheless, it has been found by [Brooks et al. \(1998\)](#) and [Bost et al. \(2001\)](#) that steranes and hopanes degradation don't follow the same biochemical pathway but are results of a complex interplay of multiple microbial reactions. As a consequence the presence of both evidences of steranes and hopanes biodegradation is rare in most of altered oils ([Peters et al., 2005](#)).

A ternary plot of carbon number homologues is presented in Figure 5 c, and a small variation between samples is evident, but

Table 1 - Raman parameters derived from spectra deconvolution. See methodology section for more details on the fitting approach.

Graphitic Carbon								
Sample	G band position	s.d.	FWMH-G	s.d.	R2	s.d.	T°C	s.d.
S14	1588.63	1.77	32.70	2.04	0.55	0.02	396.38	10.21
S15	1583.84	2.38	29.20	1.60	0.60	0.03	374.12	12.42
S16	1593.48	2.80	36.10	2.07	0.59	0.03	379.86	11.40
S17	1589.03	1.17	34.40	1.31	0.53	0.02	403.44	9.01
S18	1588.64	1.54	46.80	4.30	0.61	0.02	369.69	9.50
Disordered Carbon								
S15F	1609.35	9.56	81.64	14.31	-	-	-	-
S17	1606.20	7.75	81.05	8.01	-	-	-	-

the samples cluster in the same region indicating they are from the same source.

In combination, the biomarker parameters indicate a relatively low thermal maturity. The sterane ratio indicate an early oil window thermal maturity, whereas hopane ratio indicate a slightly higher thermal maturity (Fig. 5b and d). This is a relatively mild thermal maturity, particularly compared to the host rock, and in a classical source rock context would equate to a vitrinite reflectance of ~ 0.8 %Vr (based on comparison chart in Killops & Killops, 2005).

Fluid inclusions and Cathodoluminescence

Quartz was sampled from centimetre-scale veins folded with a NE-verging direction. CL observations show that all samples are pervasively cut by a younger generation of quartz characterized by bright CL colours (Figs. 6b,c and d) and often by syntaxial growth (Fig. 6b and c). Such features are present in all samples but are more pervasive in samples SF3 and SF4.

The petrographic characteristics and homogenization temperatures of different fluid inclusion populations reflects different quartz generations. Inclusions in the younger quartz generation (Type 1 inclusion in Table 3 and Fig. 6a and e) are bigger and occur as trails or along the edge of new crystals (Fig. 6e). Homogenization temperatures vary between 200 and 280°C (Table 3). T_H for each samples are plotted on histograms in Fig. 6a. Fluid inclusions in quartz minerals outside the youngest veins (Type 2 inclusions Tab. 3 and Fig. 6a and e) occur as isolated clusters of two phases (aqueous liquid + vapour) with dimensions generally less than 10 μ m. Their homogenization temperatures (T_H) are consistently above 300 °C.

DISCUSSION

Characterization of carbon material and fluids temperatures

Metapelites from the basement rocks of Monti Romani, in southern Tuscany, are known to be rich in organic matter that has been previously considered to be present in the form of graphitic carbon (Moretti et al., 1990; Elter & Pandeli, 1991). Nevertheless, detailed observations show that the carbonaceous materials exhibit different textures (Fig. 3) and different structural ordering

and composition, as revealed by Raman spectroscopy (Fig. 2 ad Tab. 1) and GC-MS analyses (Figs. 4 and 5 and Tab. 2).

Graphitic carbon occurs in clay-rich bands and its Raman temperatures range between 370 and 405°C comparable with greenschist metamorphic facies, attained during prograde metamorphism in the Alpine orogenesis (Funicello et al., 1984). Amorphous (disordered) carbon was detected in samples S15F and S17 in the form of dark films and nodules (Figs. 2c and 3c), suggesting fluid mobilization and redeposition (Lindgren & Parnell, 2006). Raman spectral parameters like the FWMH-G or the G band position suggest low maturity rank (i.e. diagenesis, Table 1). Nevertheless, some features such as the high intensity of bands in the “saddle” (i.e. Dr and Gl bands) between D and G bands together with the presence of bands in the second order, are not common in diagenetic spectra and can be found only in amorphous carbon matured under very fast heating rates as found near intrusions (Muirhead et al., 2017), in charcoals (Deldicque et al., 2016), in industrial black carbon (diesel soot, Sadezky et al., 2005) or in solid bitumen collected from mineralized hydrothermal veins (Jehlička et al., 2003; Sokol et al., 2014). Of these possibilities, the presence of solid bitumen is more likely in this case, given that GC-MS analyses highlight the presence of biodegraded hydrocarbons. Biodegradation removes lighter hydrocarbons, leaving high viscosity oils (i.e. bitumen) but with still the potential to migrate along fractures towards the surface.

A third group of carbon material in which the amorphous carbon spectrum is overwhelmed by fluorescence was also observed and can be associated to the biological products detected by GC-MS analyses (mosses or other endoliths) or liquid hydrocarbons.

Petrographic and fluid inclusion analyses outline the presence of two phases of quartz generation associated with different homogenization temperatures. The higher homogenization temperatures are interpreted as re-equilibration of metamorphic temperatures probably during retrograde phases and exhumation, while the young quartz generation and relative low T_H temperatures more likely relate to the recent phases of hydrothermal activity. Given that hydrothermal fluids start to circulate after the uplift of the area, T_H can be considered as representative of the fluids temperatures without any pressure correction. This range of temperatures is similar to those found by other authors in similar hydrothermal setting in nearby areas in Southern Tuscany (e.g.

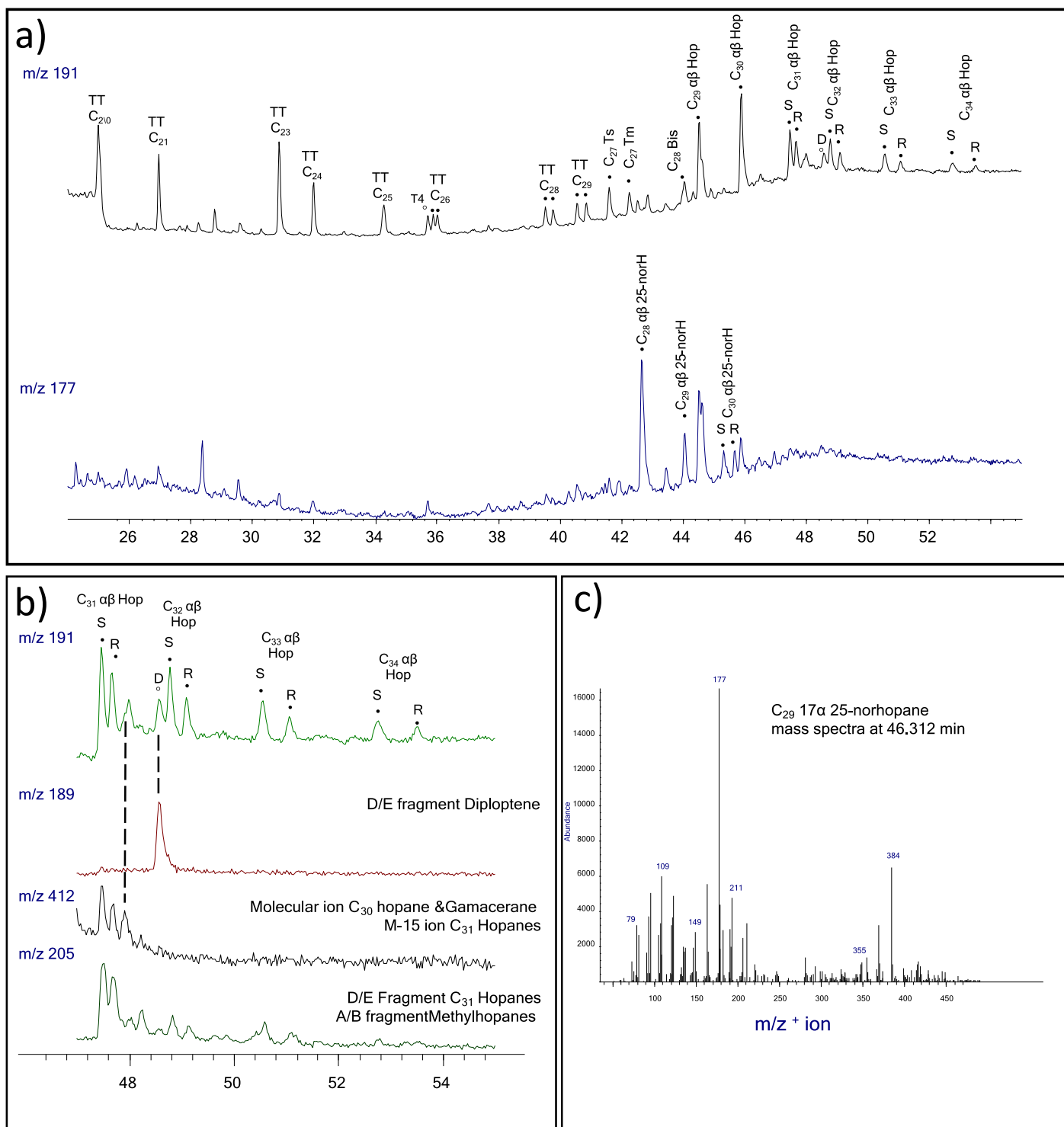


Fig. 4 - a) Ion chromatograms for m/z 191 and 177 for sample S15 showing identification of hopanes and norhopanes; b) Ion chromatograms for m/z 191, 189, 412 and 205 for sample S15 showing identification of hopanes and methylhopanes, diploptene, gammacerane; c) C₂₉ 17α 25-norhopane mass spectra at 46.312 min.

Boccheggiano fault - Liotta et al., 2010; Rossetti et al., 2011; Amiata - Brogi et al., 2011).

A model for generation and migration of hydrocarbons

GC-MS, Raman and optical analyses, demonstrate the presence of migrated hydrocarbons into the basement rocks, despite there being no productive source rocks known in the

area or nearby. Organic carbon in the closest metapelites is in the anthracitic stage with no hydrocarbon potential, while the main source rocks in the Northern Apennine are located far to the north in the Umbria-Marche domain (Oppo et al., 2013). In Tuscany the only occurrence of light hydrocarbon (methane) is known from a lignite level in the Ribolla Basin (Bencini et al., 2012). More in general, upper Tortonian lignites are known to be present in most

Table 2 - Measured biomarkers values. C_{30} Hop/Dip = C_{30} $\alpha\beta$ hopane/diploptene; Hop 22S = $C_{31}17\alpha$, 21 β (H) 22S/ $C_{31}17\alpha$, 21 β (H) 22S + $C_{31}17\alpha$, 21 β (H) 22R hopane; Ts/Ts+Tm = $C_{27}18\alpha$ (H)-22,30-trisnorhopane/($C_{27}18\alpha$ (H)-22,30-trisnorhopane + $C_{27}17\alpha$ (H)-22,30-trisnorhopane); Ster 20S = $C_{29}5\alpha$, 14 α , 17 α (H) 20S/ $C_{29}5\alpha$, 14 α , 17 α (H) 20S + $C_{29}5\alpha$, 14 α , 17 α (H) 20S sterane; The sterane compositions C_{27} $\alpha\alpha\alpha$ R, C_{28} $\alpha\alpha\alpha$ R and C_{29} $\alpha\alpha\alpha$ R were obtained by dividing the height of one homologue by the sum of the other 27-29 homologues.

Sample	measured on m/z 191									measured on m/z 217				
	EOM ($\mu\text{g g}^{-1}$)	%Sats	%Arom	%Polar	TT C_{23}/C_{30} Hop	C_{29} Hop/ C_{28} 25-norHop	C_{30} Hop/ Dip	Hop 22S	Ts/Ts+Tm	Ster 20S	$\alpha\beta\beta/\alpha\alpha\alpha+\alpha\beta\beta$	C_{27} $\alpha\alpha\alpha$ R	C_{28} $\alpha\alpha\alpha$ R	C_{29} $\alpha\alpha\alpha$ R
S15	0.15	1.2	1.2	97.6	0.63	0.98	2.91	0.60	0.58	0.40	0.44	0.30	0.18	0.52
S15F	0.65	17.6	5.9	76.5	0.91	0.00	1.95	0.60	0.53	0.42	0.48	0.41	0.16	0.42
S14	0.05	50.0	25.0	25.0	0.84	3.62	2.24	0.62	0.58	0.45	0.46	0.31	0.18	0.51
S16	0.06	66.7	16.7	16.7	0.77	4.42	2.44	0.57	0.62	0.46	0.49	0.34	0.24	0.42
S17	0.18	16.7	16.7	66.7	0.86	6.54	1.86	0.52	0.48	0.37	0.47	0.31	0.19	0.50
S18	0.09	10.0	80.0	10.0	0.56	6.65	1.67	0.52	0.52	0.43	0.44	0.32	0.19	0.49

Table 3 - Fluid inclusion average homogenization temperatures.

Samples	T_H (°C) Type 1	T_H (°C) Type 2
SF1	276	338
SF2	211	317
SF3	240	321
SF4	213	325

of the neogenic basin in Southern Tuscany (i.e., Ribolla, Baccinello, Radicofani and Albegna basins, [Staccioli et al., 2001](#); [Bossio et al., 2003](#); [Pascucci et al., 2006](#); [Bencini et al., 2012](#); [Cirilli et al., 2016](#)). They generally occur at shallow depth overlaid by few hundred of meters of Plio-quadernary cover and only in the Ribolla basin the condition for hydrocarbon generation were met with a relatively high burial (~ 1000 m) and an extremely high heat flow due to the closeness to the geothermal Larderello field ([Bencini et al., 2012](#)). Nevertheless, a migration from the Ribolla basin is unlikely given the distance (more than 50 km) and the thermal maturity in the oil window depicted by hopanes and steranes ratios in our samples (Figs. 5b and d).

GC-MS analyses show that hydrocarbons are present in all samples across the studied outcrop, with the highest concentration (higher EOM in Table 3) and the only evidence in Raman analyses of amorphous carbon, in samples S15, S15F and S17, that are located along extensional structural elements (Fig. 2a). Fractures and faults related to the post-orogenic extension that started in the middle-late Miocene ([Berardi et al., 2016](#)) and led to the opening of the Tafone Basin, were thus probably a preferential path for hydrocarbon migration. Furthermore, the same structural elements were the carriers of the intense hydrothermal circulation developed as a consequence of the emplacement at shallow depth of magmatic products belonging to the Tuscan Magmatic Province ([Dini et al., 2005](#); [Rossetti et al., 2008](#); [Morteani et al., 2011, 2017](#)). The association between quartz mineralization and carbon material (Fig. 3) suggest a role of the fluids in the transport, maturation and likely genesis of the hydrocarbons. During their path toward the surface the hot fluids could have reacted with the immature organic matter of the late organic rich sediments, probably the Tortonian-

early Messinian ([Cornamusini et al., 2011](#)), or at least the Santa Croce Unit (see discussion below), to hydrothermally generate hydrocarbons. Hydrothermal generation is known to occur as a consequence of the interaction between organic matter with high temperature fluids and has been widely documented, both near oceanic spreading centers ([Simoneit, 1990](#)) and in continental rift systems ([Zárate-Del Valle & Simoneit, 2005](#)). Formation and migration of hydrothermal petroleum is known to occur rapidly (days-years), in a higher temperature range than conventional oils (from about 60 °C to more than 400 °C) and from source rocks with high to very low TOC content ([Peter et al., 1991](#); [Simoneit, 1994](#)). Considering the fluid inclusion homogenization temperatures (180-280 °C, Fig. 6a), it is reasonable that generation could have occurred in a short-time (years) of repeated hydrothermal pulses that have imparted sufficient energy to drive isomerisation reactions of an immature kerogen ([Tsang et al., 2020](#)) and led to the measured thermal maturity (i.e. oil window; Fig. 5b and d and Tab. 3).

Hydrothermal oils share similarities with conventional oils, such as the presence of the full range of n-alkanes, isoprenoid hydrocarbons and biomarkers like mature 17 α (H)-hopanes and steranes, while have been reported to differ in the relative abundance of polycyclic aromatic hydrocarbons (PAH) that become dominant for temperatures higher than 350°C ([Peter et al., 1991](#); [Simoneit & Kvenvolden, 1994](#)). The occurrence of both liquid and solid (i.e bitumen) hydrocarbons within quartz (Figs. 3b,c and d) associate to Raman spectra that resemble those ones of hydrothermal bitumen (see discussion above) strengthens the hypothesis of a hydrothermal generation.

According to biomarker data in the ternary plot in Figure 5c, all samples seem to cluster in the same region, suggesting an origin from a common source rock composed of a mix of terrestrial and marine organic matter that could agree to the brackish lagoon to shallow marine origin of the late Miocene sediments that fill the Tafone Graben. Given uncertainties linked to the ternary plot of Fig. 5c, a generation from the underneath Santa Croce Unit (Ligurian) cannot be discarded. Nevertheless, Internal Ligurian Units in Tuscany ([Rossetti et al., 2011](#); [Marroni et al., 2015](#)) and more in general in the northern Appennine ([Corrado et al.,](#)

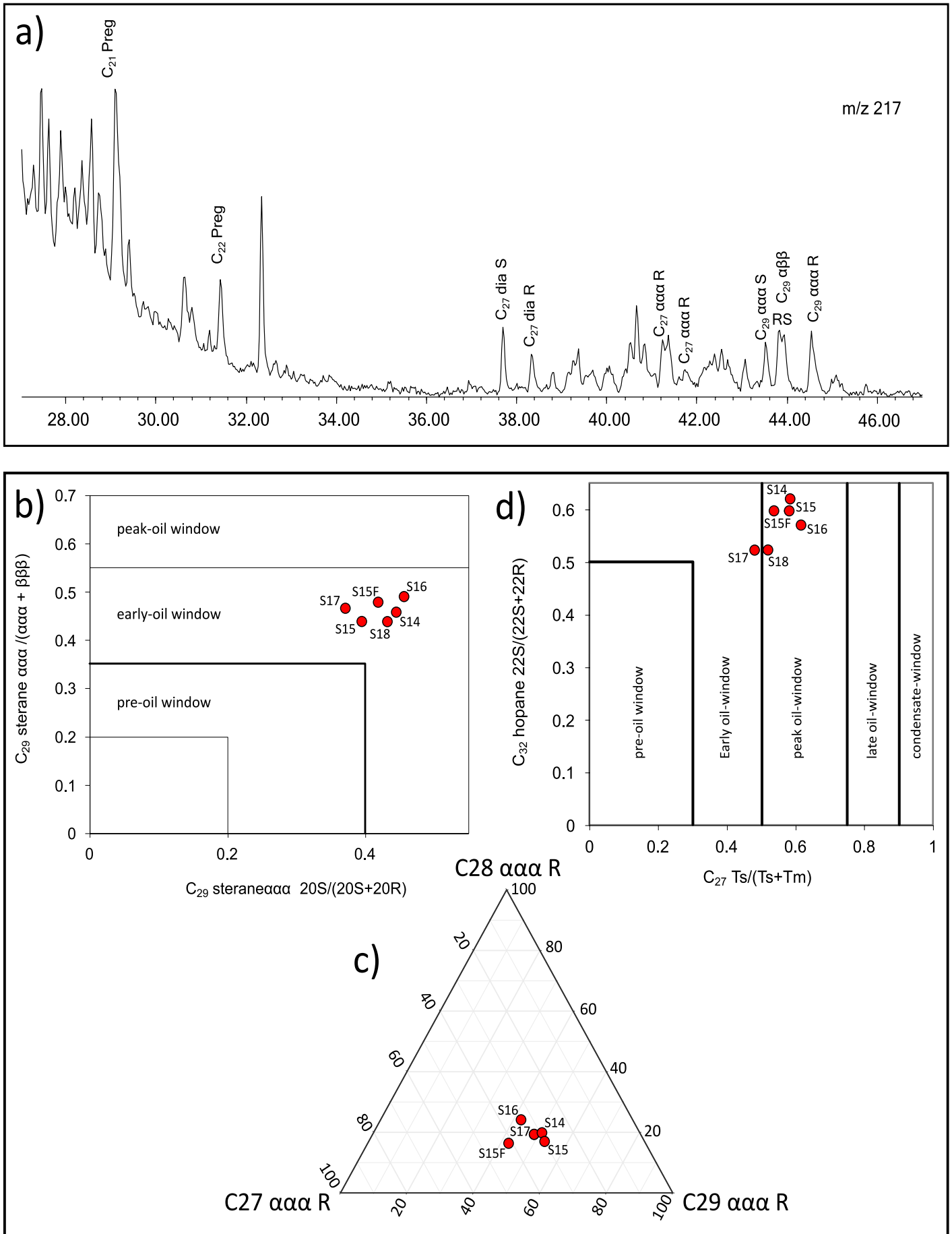


Fig. 5 - a) Ion chromatograms for m/z 217 for sample S17 showing identification of diasterane and sterane; b) 20S sterane vs $\alpha\beta / \alpha\alpha + \beta\beta$ maturity diagram; c) ternary C_{27} , C_{28} , C_{29} diagram; d) 22 hopane vs Ts/Ts+Tm maturity diagram.

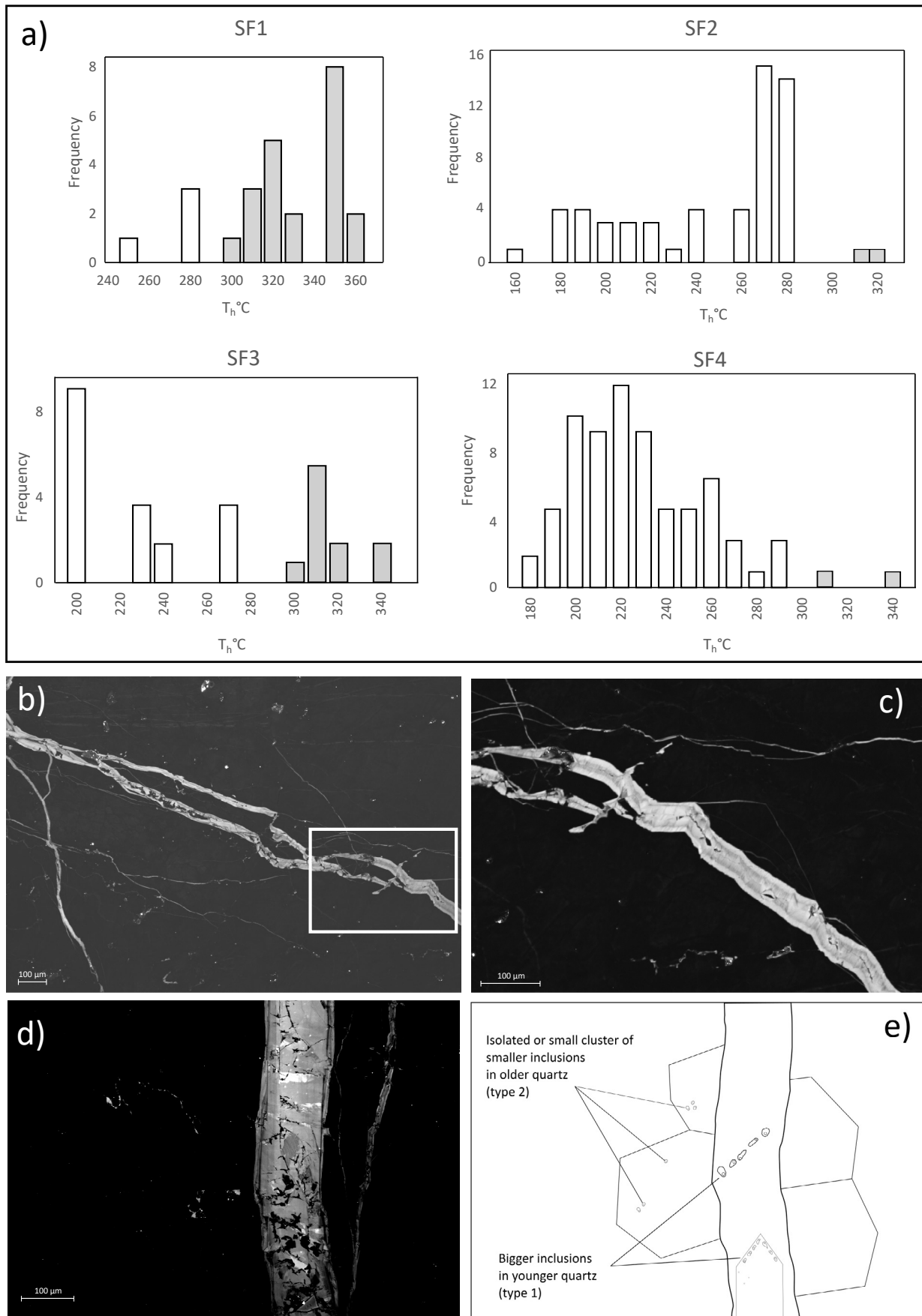


Fig. 6 - a) Homogenization temperature histograms from fluid inclusion analyses of samples SF1, SF2, SF3 and SF4. White and grey bins indicate respectively type 1 and type 2 inclusions **b)** CL image showing the relationship between young quartz (brightest) into old quartz represented by the dark background. **c)** Close-up of the inset of image **b)** showing the syntaxial growth of the vein with different CL brightness, indicating different stages of mineralization. **d)** CL image showing the relationship between young quartz (brightest) into old quartz represented by the dark background. **e)** sketch showing different fluid inclusion populations in quartz.

2010; Dellisanti et al., 2010) are known to have suffered deep diagenetic to low metamorphic (anchizone) condition and this is not in agreement with hopanes and in particular steranes thermal maturity ratios (Tab. 2). Once generation occurred, given the low permeability in the hanging wall, hydrocarbons probably migrated toward the fractured basement rocks of the footwall (Fig. 7).

After migration, oil was degraded by microbial activity as testified by the presence of 25-norhopanes. 25-norhopanes form through the microbial removal of the methyl group at C-10 from hopanes during biodegradation. This is a temperature-controlled process that occurs in anaerobic burial conditions, thus perhaps below 100 m depth and was never found to occur at temperatures higher than 80 °C (Wilhelms et al., 2001). Considering the present day geothermal gradient of 50 °C/km (Della Vedova et al., 2001), this means that biodegradation occurred to a depth of about 1500 m as shown in Fig. 7. Both degraded and not hydrocarbon were finally brought to the surface during one last hydrothermal pulses (Fig. 7).

It is worth to state that, as an alternative hypothesis to justify the presence of bitumen in the Amiata region, Rimondi et al. (2015) propose the presence of an underlying organic-rich shale. Nevertheless, we have any knowledge of carbon-rich shales below the Tuscan or metamorphic series. Moreover, this interpretation, imply a questionable allochthonous origin of the metamorphic units that, perhaps in the nearby Amiata region are known to be

autochthonous by deep drilling for geothermal purposes (Carmignani et al., 1994; Brogi, 2008).

Implication for the Southern Tuscany ore district

The association of hydrocarbons with ore deposits is a worldwide recognized phenomenon (Parnell, 1993). In particular, it was demonstrated that in hydrothermal environments, liquid hydrocarbons, bitumen and the remaining kerogen can act as strong reducing agents during ore (in particular sulphides) mineralization (Peabody, 1993). The Tafone Basin hosts important stibnite deposits along the faults that border the graben at the contact between the basement rocks with the limestones and dolostones of the Tuscany series. The results from this work highlight that the hydrocarbons circulated in the basement rocks during hydrothermal activity and thus could have played a key role in the sulphide mineralization of the area.

Interestingly, several authors report the presence of solid hydrocarbons in the Mt. Amiata region (Arisi Rota & Vighi, 1971; Rimondi et al., 2015) that is one of the main ore district in Southern Tuscany, suggesting they could have contributed to the mineralization process. The origin of such bitumen has never been explained, so the model provided in this work could be tentatively exported to similar areas.

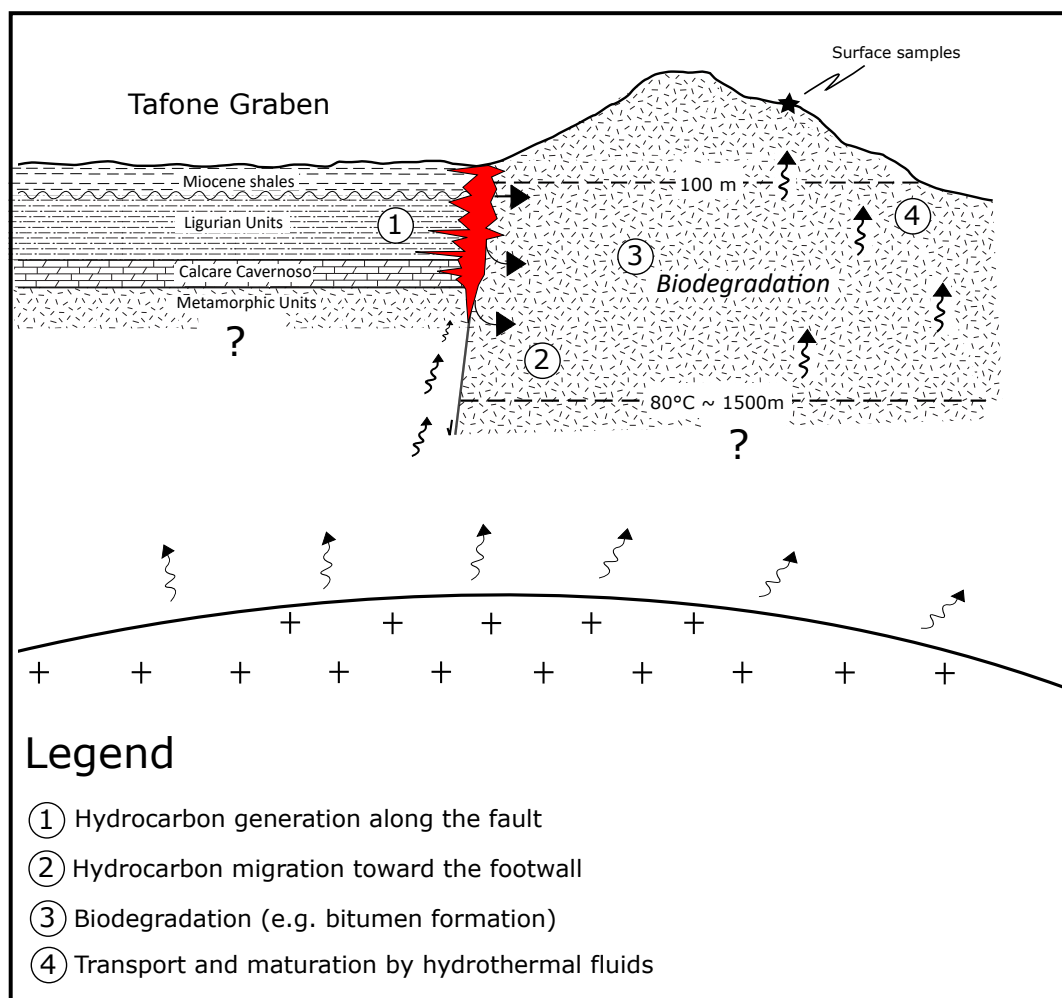


Fig. 7 - Conceptual model (not to scale) for generation, degradation and migration of hydrocarbons in the Tafone area. The figure shows the path of hydrothermal fluids from the heat source represented by a cooling intrusion. Red colour around the fault indicates hot fluid circulation around the fault that could generate hydrocarbons when in contact with organic-rich Miocene rocks, while arrows show the possible path of migration from the hanging wall toward and inside the footwall up to the surface. Depth interval for biodegradation was calculated according to the present day geothermal gradient of 50°C/km following the regional map of Della Vedova et al. (2001).

CONCLUSIONS

We report the occurrence of hydrocarbons in hydrothermally altered metamorphic rocks of Monti Romani in Southern Tuscany. The association of amorphous carbon and hydrocarbons with high temperature fluid inclusions in mineralized veins suggests a hydrothermal origin for the hydrocarbons. The presence of 25-norhopanes shows that microbial biodegradation occurred at depth in the basement rocks, confirming that hydrocarbon-bearing basement rocks can be a favourable habitat for microbial activity (Marynowski et al., 2011; Parnell et al., 2017).

The genetic model for hydrothermal generation and migration of hydrocarbons proposed in this work could explain the presence of hydrocarbons in others geothermal areas of Southern Tuscany which may have played a role in ore mineralization.

ACKNOWLEDGEMENTS

The work has been possible thanks to the Royal Society of Edinburgh and Accademia dei Lincei Bilateral visit grant, to which GC-MS, fluid inclusions and CL data have been produced. Alex Brasier and John Still are acknowledged for help with preparing CL images. Sveva Corrado is kindly acknowledge for organization of the first field trip and stimulating discussion in the first phases of the work. We thank Claudia Romano for the use of EVPLab laboratories for Raman spectroscopic analyses. Gabriele Berardi is acknowledged for help during sampling and Amalia Spina and Andrea Brogi for fruitful discussions and suggestions. Editor in chief Federico Rossetti, the Associated Editor Orlando Vaselli, Fabio Massimo Petti, Roberto Galimberti and two anonymous reviewer are acknowledge for stimulating comments and suggestions during manuscript revisions. The work was funded by the University of Aberdeen.

REFERENCES

- Acocella V. & Funicello R. (2006) - Transverse systems along the extensional Tyrrhenian margin of central Italy and their influence on volcanism. *Tectonics*, 25(2), 1-24.
- Al-Hajeri M.M. & Bowden S.A. (2018) - Origin of oil geochemical compositional heterogeneity in the Radhuma and Tayarat formations heavy oil carbonate reservoirs of Burgan Field, south Kuwait. *Arabian Journal of Geosciences*, 11, 1-15.
- Anderson R.B., Kölbl H. & Rálek M. (1984) - The Fischer-Tropsch Synthesis. Academic Press, Orlando, 311 pp.
- Arisi Rota F. & Vighi L. (1971) - Le mineralizzazioni a pirite e a solfuri misti. *Rendiconti Società Italiana di Mineralogia & Petrografia*, 27, 370-422.
- Armiento G., Nardi E., Lucci F., De Cassan M., Della Ventura G., Santini C., Petrini E. & Cremisi C. (2017) - Antimony and arsenic distribution in a catchment affected by past mining activities: influence of extreme weather events. *Rendiconti Lincei*, 28 (2), 303-315.
- Barchi M. (2010) - The Neogene-Quaternary evolution of the Northern Apennines: crustal structure, style of deformation and seismicity. *Journal of the Virtual Explorer*, 36.
- Bencini R., Bianchi E., De Mattia R., Martinuzzi A., Rodorigo S. & Vico G. (2012) - Unconventional Gas in Italy: the Ribolla Basin. AAPG International Conference & Exhibition, 80203, 27.
- Bennett B., Fustic M., Farrimond P., Huang H. & Larter S.R. (2006) - 25-Norhopanes: formation during biodegradation of petroleum in the subsurface. *Organic Geochemistry*, 37, 787-797.
- Berardi G., Vignaroli G., Billi A., Rossetti F., Soligo M., Kele Oruçbaykara M., Bernasconi S.M., Castorina F., Tecce F. & Shen C.C. (2016) - Growth of a Pleistocene giant carbonate vein and nearby thermogene travertine deposits at Semproniano, southern Tuscany, Italy: Estimate of CO₂ leakage. *Tectonophysics*, 690, 219-239.
- Beysac O., Goffé B., Chopin C. & Rouzard J.N. (2002) - Raman spectra of carbonaceous material in metasediments: a new geothermometer. *Journal of metamorphic Geology*, 20(9), 859-871.
- Biagioni C., Silvia M. & Pasero M. (2017) - New data on metacinnabar from Tuscany (Italy). *Atti della Società Toscana di Scienze Naturali*, 74, 13-19, <https://doi.org/10.2424/ASTSN.M.2017.14>.
- Bossio A., Foresi L.M., Mazzei R., Salvatorini G., Sandrelli F., Bilotti M., Colli A. & Rossetto R. (2003) - Geology and stratigraphy of the southern sector of the Neogene Albegna River Basin (Grosseto, Tuscany, Italy). *Geologica Romana*, 37, 165-173.
- Bost F.D., Frontera-Suau R., McDonald T.J., Peters K.E. & Morris P.J. (2001) - Aerobic biodegradation of hopanes and norhopanes in Venezuelan crude oils. *Organic Geochemistry*, 32(1), 105-114.
- Brobst D.A. (1973) - United States mineral resources. *Geological Survey Professional Paper 820*. Pratt, W.P. (Ed.). United States, 13(4), 722 pp.
- Brogi A. (2008) - The Triassic and Palaeozoic successions drilled in the Bagnore geothermal field and Poggio Nibbio area (Monte Amiata, Northern Apennines, Italy). *Bollettino della Società Geologica Italiana*, 127, 599-613.
- Brogi A. & Giorgetti G. (2012) - Tectono-metamorphic evolution of the siliciclastic units in the Middle Tuscan Range (inner Northern Apennines): Mg-carpholite bearing quartz veins related to syn-metamorphic syn-orogenic foliation. *Tectonophysics*, 526, 167-184.
- Brogi A., Fabbrini L. & Liotta D. (2011) - Sb-Hg ore deposit distribution controlled by brittle structures: the case of the Selvena mining district (Monte Amiata, Tuscany, Italy). *Ore Geology Reviews*, 41, 35-48.
- Brogi A., Caggianelli A., Liotta D., Zucchi M., Spina A., Capezzuoli E., Casini A. & Buracchi E. (2021) - The Gavorrano Monzogranite (Northern Apennines): An Updated Review of Host Rock Protoliths, Thermal Metamorphism and Tectonic Setting. *Geosciences*, 11(3), 124.
- Brooks P.W., Fowler M.G. & Macqueen R.W. (1988) - Biological marker and conventional organic geochemistry of oil sands/heavy oils, Western Canada Basin. *Organic Geochemistry*, 12, 519-538.
- Carmignani, L., Decandia, F. A., Fantozzi, P. L., Lazzarotto, A., Liotta, D., & Meccheri, M. (1994) - Tertiary extensional tectonics in Tuscany (northern Apennines, Italy). *Tectonophysics*, 238(1-4), 295-315.
- Cipriani C. & Tanelli G. (1983) - Risorse minerarie ed industria estrattiva in Toscana. *Atti e Memorie dell'Accademia Toscana di Scienze e Lettere'La Colombaria*, 48, 241-282.
- Cirilli O., Benvenuti M., Carnevale G., Casanovas-Villar I., Delfino M., Furiò M., Papini M., Villa A. & Rook L. (2016) - Fosso della Fittiaia: the oldest Tusco-Sardinian late Miocene endemic vertebrate assemblage (Baccinello-Cinigiano Basin, Tuscany, Italy). *Rivista Italiana di Paleontologia e Stratigrafia*. 122(2), 13-34.
- Clifton C.G., Walters C.C. & Simoneit B.R.T. (1990) - Hydrothermal petroleum from Yellowstone National Park, Wyoming, USA. *Applied Geochemistry*, 5, 169-191.
- Connan J. (1984) - Biodegradation of crude oils in reservoirs. *Advances in petroleum geochemistry*, 1, 229-335.
- Cornamusini G., Foresi L.M., Massa G., Bonciani F., Callegari I., Da Prato S. & Ielpi A. (2011) - The Miocene successions of the Fiora Hills: considerations about the development of the minor basins of Southern Tuscany. *Italian Journal of Geosciences*, 130, 404-424.

- Corrado S., Aldega L. & Zattin M. (2010) - Sedimentary vs. tectonic burial and exhumation along the Apennines (Italy) paper 15. In: Beltrando M., Peccerillo A., Mattei M., Conticelli S. & Doglioni C., *The Geology of Italy. Journal of Virtual Explorer*, 36.
- Della Vedova B., Bellani S., Pellis G., & Squarci P. (2001) - Deep temperatures and surface heat flow distribution. In *Anatomy of an orogen: the Apennines and adjacent Mediterranean basins*. Springer, Dordrecht, 65-76.
- Deldicque D., Rouzaud J.N. & Velde B. (2016) - A Raman - HRTEM study of the carbonization of wood: A new Raman-based paleothermometer dedicated to archaeometry. *Carbon*, 102, 319-329.
- Dellisanti F., Pini G. A. & Baudin F. (2010) - Use of T max as a thermal maturity indicator in orogenic successions and comparison with clay mineral evolution. *Clay minerals*, 45(1), 115-130.
- Dessau G., Duchi G. & Stea B. (1972) - Geologia e depositi minerari della zona Monti Romani-Monteti (Comuni di Manciano e Capalbio (Grosseto) ed Ischia Di Castro (Viterbo). *Memorie della Società Geologica Italiana*, 11, 217-260.
- Dini A., Gianelli G., Puxeddu M. & Ruggieri G. (2005) - Origin and evolution of Pliocene–Pleistocene granites from the Larderello geothermal field (Tuscan Magmatic Province, Italy). *Lithos*, 81, 1-31.
- Elter F.M. & Pandeli E. (1991) - Structural features of the metamorphic Paleozoic-Triassic sequences in deep geothermal drillings of the Monte Amiata area (SE Tuscany, Italy). *Bollettino della Società Geologica Italiana*, 110, 511-522.
- Ferralis N., Matys E.D., Knoll A.H., Hallmann C. & Summons R.E. (2016) - Rapid, direct and non-destructive assessment of fossil organic matter via microRaman spectroscopy. *Carbon*, 108, 440-449.
- Funciello R., Salvini F. & Wise D.U. (1984) - Deformational history of basement exposures along the Fiora river, central Italy. *Bollettino della Società Geologica italiana*, 103, 491-501.
- Gurgey K., Simoneit B.R.T., Bati Z., Karamanderesi I.H. & Varol B. (2007) - Origin of petroliferous bitumen from the Buyuk Menderes-Gediz geothermal graben system, Denizli-Saraykoy, western Turkey. *Applied Geochemistry*, 22, 1393.
- Holdsworth R.E., Trice R., Hardman K., Mccaffrey K.J.W., Morton A., Frei D., Dempsey E., Bird A. & Rogers S. (2020) - The nature and age of basement host rocks and fissure fills in the Lancaster field fractured reservoir, West of Shetland. *Journal of the Geological Society*, 177(5), 1057-1073.
- Jehlička J., Urban O. & Pokorný J. (2003) - Raman spectroscopy of carbon and solid bitumens in sedimentary and metamorphic rocks. *Spectrochimica Acta Part A: Molecular and Biomolecular Spectroscopy*, 59, 2341-2352.
- Jolivet L., Faccenna C., Goffè B., Mattei M., Rossetti F., Brunet C., Storti F., Funciello R., Cadet J.P., D'agostino N. & Parra T. (1998) - Midcrustal shear zones in postorogenic extension: example from the northern Tyrrhenian Sea. *Journal of Geophysical Research: Solid Earth*, 103, 12123-12160.
- Killops S.D. & Killops V.J. (2005) - *Introduction to Organic Geochemistry*. second ed., Blackwell publishing, Oxford, 404 pp.
- Klemm D.D. & Neumann N. (1984) - Ore-controlling factors in the Hg-Sb province of southern Tuscany, Italy. In: *Syngenesi and Epigenesis in the Formation of Mineral Deposits*. Springer, Berlin, Heidelberg, 482-503.
- Kontorovich A.E., Bortnikova S.B., Karpov G.A., Kashirtsev V.A., Kostyreva E.A. & Fomin A.N. (2011) - Uzon volcano caldera (Kamchatka): A unique natural laboratory of the present-day naphthide genesis. *Russian Geology and Geophysics*, 52, 768-772.
- Landes K.K., Amoroso J.J., Charlesworth J.L.J., Heany F. & Lesperance P.J. (1960) - Petroleum resources in basement rocks. *AAPG Bulletin*, 44, 1682-1691.
- Li C.Z. (2007) - Some recent advances in the understanding of the pyrolysis and gasification behaviour of Victorian brown coal. *Fuel*, 86, 1664-1683.
- Lindgren P. & Parnell J. (2006) - Petrographic criteria for fluid mobility of graphitic carbon in terrestrial and extraterrestrial samples. *Journal of Geochemical Exploration*, 91, 126-129.
- Liotta D., Ruggieri G., Brogi A., Fulignati P., Dini A. & Nardini I. (2010) - Migration of geothermal fluids in extensional terrains: the ore deposits of the Boccheggiano-Montieri area (southern Tuscany, Italy). *International Journal of Earth Sciences*, 99, 623-644.
- Lollar B.S., Westgate T.D., Ward J.A., Slater G.F. & Lacrampe-Couloume G. (2002) - Abiogenic formation of alkanes in the Earth's crust as a minor source for global hydrocarbon reservoirs. *Nature*, 416, 522-524.
- Lucca A., Storti F., Molli G., Muchez P., Schito A., Artoni A., Balsamo F., Corrado S. & Mariani E.S. (2019) - Seismically enhanced hydrothermal plume advection through the process zone of the Compione extensional Fault, Northern Apennines, Italy. *GSA Bulletin*, 131(3-4), 547-571.
- Marroni M., Pandeli E., Pandolfi L. & Catanzariti R. (2015) - Updated picture of the Ligurian and Sub-Ligurian units in the Mt. Amiata area (Tuscany, Italy): elements for their correlation in the framework of the Northern Apennines. *Italian Journal of Geosciences*, 134(2), 200-218.
- Marynowski L., Kurkiewicz S., Rakociński M. & Simoneit B.R.T. (2011) - Effects of weathering on organic matter: I. Changes in molecular composition of extractable organic compounds caused by paleoweathering of a Lower Carboniferous (Tournaisian) marine black shale. *Chemical Geology*, 285, 144-156.
- Molli G. (2008) - Northern Apennine–Corsica orogenic system: an updated overview. *Geological Society, London, Special Publications*, 298, 413-442.
- Molli G., Brogi A., Caggianelli A., Capezzuoli E., Liotta D., Spina A. & Zibra I. (2020) - Late Palaeozoic tectonics in Central Mediterranean: a reappraisal. *Swiss Journal of Geosciences*, 113(1), 1-32.
- Moretti A., Meletti C. & Ottria G. (1990) - Studio stratigrafico e strutturale dei Monti Romani (GR-VT)-1: Dal Paleozoico all'orogenesi alpida. *Bollettino della Società Geologica Italiana*, 109, 557-581.
- Morteani G., Ruggieri G., Möller P. & Preinfalk C. (2011) - Geothermal mineralized scales in the pipe system of the geothermal Piancastagnaio power plant (Mt. Amiata geothermal area): a key to understand the stibnite, cinnabarite and gold mineralization of Tuscany (central Italy). *Mineralium Deposita*, 46, 197-210.
- Morteani G., Voropaev A. & Grinenko V. (2017) - Relation of stibnite mineralisation and geothermal fluids in southern Tuscany (central Italy): an isotope (C, O, H, S) and Rare Earth Element study. *Neues Jahrbuch für Mineralogie-Abhandlungen*, 194, 279-296.
- Muirhead D.K., Bowden S.A., Parnell J. & Schofield N. (2017) - Source rock maturation owing to igneous intrusion in rifted margin petroleum systems. *Journal of the Geological Society*, 174(6), 979-987.
- Nirrengarten M., Mohn G., Schito A., Corrado S., Gutiérrez-García L., Bowden S.A. & Despinois F. (2020) - The thermal imprint of continental breakup during the formation of the South China Sea. *Earth and Planetary Science Letters*, 531, 115972.
- Oppo D., Capozzi R. & Picotti V. (2013) - A new model of the petroleum system in the Northern Apennines, Italy. *Marine and Petroleum Geology*, 48, 57-76.

- Orlando A., Conte A.M., Borrini D., Perinelli C., Gianelli G. & Tassi F. (2010) - Experimental investigation of CO₂-rich fluids production in a geothermal area: The Mt Amiata (Tuscany, Italy) case study. *Chemical Geology*, 274, 177-186.
- Pancost R.D., Baas M., Van Geel B. & Sinninghe Damsté J.S. (2002) - Biomarkers as proxies for plant inputs to peats: An example from a sub-boreal ombrotrophic bog. *Organic Geochemistry*, 33, 675-690.
- Parnell J. (1988) - Metal enrichments in solid bitumens: a review. *Mineralium Deposita*, 23, 191-199.
- Parnell J. (1993) - Metal enrichments in bitumens from the Carboniferous of Ireland: potential in exploration for ore deposits. In: *Bitumens in Ore Deposits*. Springer, Berlin, Heidelberg, 475-489.
- Parnell J., Bowden S., Osinski G.R., Taylor C.W. & Lee P. (2008) - The transfer of organic signatures from bedrock to sediment. *Chemical Geology*, 247, 242-252.
- Parnell J., Bowden S. & Muirhead D. (2017) - Subsurface biodegradation of crude oil in a fractured basement reservoir, Shropshire, UK. *Journal of the Geological Society*, 174, 655-666.
- Pascucci V., Costantini A., Martini I.P. & Dringoli R. (2006) - Tectono-sedimentary analysis of a complex, extensional, Neogene basin formed on thrust-faulted, Northern Apennines hinterland: Radicofani Basin, Italy. *Sedimentary Geology*, 183, 71-97.
- Peabody C.E. (1993) - The association of cinnabar and bitumen in mercury deposits of the California Coast Ranges. In: *Bitumens in Ore Deposits*. Springer, Berlin, Heidelberg, 178-209.
- Peter J.M., Peltonen P., Scott S.D., Simoneit B.R.T. & Kawka O.E. (1991) - ¹⁴C ages of hydrothermal petroleum and carbonate in Guaymas Basin, Gulf of California: implications for oil generation, expulsion, and migration. *Geology*, 19, 253-256.
- Peters K.E., Walters C.C. & Moldowan J.M. (2005) - *The biomarker guide: Volume 1, Biomarkers and isotopes in the environment and human history*, 2nd Ed. Cambridge university press, Cambridge, UK, 1155 pp.
- Prahl F.G., Hayes J.M. & Xie T.M. (1992) - Diploptene: an indicator of terrigenous organic carbon in Washington coastal sediments. *Limnology and Oceanography*, 37, 1290-1299.
- Rimondi V., Chiarantini L., Lattanzi P., Benvenuti M., Beutel M., Colica A., Costagiola P., De Benedetto F., Gabbani G., Gray J. E., Pandeli E., Pattelli G., Paolieri M. & Ruggeri G. (2015) - Metallogeny, exploitation and environmental impact of the Mt. Amiata mercury ore district (Southern Tuscany, Italy). *Italian Journal of Geosciences*, 134, 323-336, <https://doi.org/10.3301/IJG.2015.02>.
- Rossetti F., Balsamo F., Villa I.M., Bouybaouenne M., Faccenna C. & Funicello R. (2008) - Pliocene–Pleistocene HT–LP metamorphism during multiple granitic intrusions in the southern branch of the Larderello geothermal field (southern Tuscany, Italy). *Journal of the Geological Society*, 165, 247-262.
- Rossetti F., Aldega L., Tecce F., Balsamo F., Billi A. & Brilli M. (2011) - Fluid flow within the damage zone of the Boccheggiano extensional fault (Larderello–Travale geothermal field, central Italy): structures, alteration and implications for hydrothermal mineralization in extensional settings. *Geological Magazine*, 148, 558-579.
- Sadezky A., Muckenhuber H., Grothe H., Niessner R. & Pöschl U. (2005) - Raman microspectroscopy of soot and related carbonaceous materials: Spectral analysis and structural information. *Carbon*, 43, 1731-1742.
- Schito A., Romano C., Corrado S., Grigo D. & Poe B. (2017) - Diagenetic thermal evolution of organic matter by Raman spectroscopy. *Organic Geochemistry*, 106, 57-67.
- Schoell M., Hwang R.J. & Simoneit B.R.T. (1990) - Carbon isotope composition of hydrothermal petroleum from Guaymas Basin, Gulf of California. *Applied Geochemistry*, 5, 65-69.
- Schutter S.R. (2003) - Occurrences of hydrocarbons in and around igneous rocks. Geological Society, London, Special Publications, 214, 35-68.
- Simoneit B.R.T. (1990) - Petroleum generation, an easy and widespread process in hydrothermal systems: an overview. *Applied Geochemistry*, 5, 3-15.
- Simoneit B.R. & Kvenvolden K.A. (1994) - Comparison of ¹⁴C ages of hydrothermal petroleum. *Organic geochemistry*, 21(5), 525-529.
- Simoneit B.R.T. (1994) - Organic matter alteration and fluid migration in hydrothermal systems. Geological Society, London, Special Publications, 78, 261-274.
- Simoneit B.R.T., Deamer D.W. & Kompanichenko V. (2009) - Characterization of hydrothermally generated oil from the Uzon caldera, Kamchatka. *Applied Geochemistry*, 24, 303-309.
- Sokol E., Kozmenko O., Smirnov S., Sokoi., Novikova S., Tomilenko A., Kokh S., Ryazanova T., Reutsky V., Bul'bak T., Vapnik Y. & Deyak M. (2014) - Geochemical assessment of hydrocarbon migration phenomena: Case studies from the south-western margin of the Dead Sea Basin. *Journal of Asian Earth Sciences*, 93, 211-228.
- Staccioli G., Sturaro A., Parvoli G. & Alberti M.B. (2001) - Chemical characterisation of lignites from Montebamboli and Ribolla (South Tuscany, Italy) and botanical suggestions of their plant source material. *Flora Mediterranea*, 11, 419-434.
- Tassi F., Fiebig J., Vaselli O. & Nocentini M. (2012) - Origins of methane discharging from volcanic-hydrothermal, geothermal and cold emissions in Italy. *Chemical Geology*, 310, 36-48.
- Tsang M.Y., Bowden S.A., Wang Z., Mohammed A., Tonai S., Muirhead D., Yang K., Yamamoto Y., Kamiya N., Okutsu N., Hirose T., Kars M., Shobotz F., Ijiri A., Yamada Y., Kubo Y., Morono Y., Inagaki F., Heuer V. & Hinrich K. U. (2020) - Hot fluids, burial metamorphism and thermal histories in the underthrust sediments at IODP 370 site C0023, Nankai Accretionary Complex. *Marine and Petroleum Geology*, 112, 104080 .
- Venkatesan M.I., Ruth E., Rao P.S., Nath B.N. & Rao B.R. (2003) - Hydrothermal petroleum in the sediments of the Andaman Backarc Basin, Indian Ocean. *Applied Geochemistry*, 18, 845-861.
- Wilhelms A., Larter S.R., Head I., Farrimond P., Di-Primio R. & Zwach C. (2001) - Biodegradation of oil in uplifted basins prevented by deep-burial sterilization. *Nature*, 411(6841), 1034-1037.
- Yamanaka T., Ishibashi J. & Hashimoto J. (2000) - Organic geochemistry of hydrothermal petroleum generated in the submarine Wakamiko caldera, southern Kyushu, Japan. *Organic Geochemistry*, 31, 1117-1132.
- Zárate-Del Valle P.F. & Simoneit B.R.T. (2005) - Hydrothermal bitumen generated from sedimentary organic matter of rift lakes–Lake Chapala, Citala Rift, western Mexico. *Applied geochemistry*, 20, 2343-2350.
- Zárate-Del Valle P.F., Rushdi A.I. & Simoneit B.R.T. (2006) - Hydrothermal petroleum of Lake Chapala, Citala Rift, western Mexico: Bitumen compositions from source sediments and application of hydrous pyrolysis. *Applied geochemistry*, 21, 701-712.